An Analysis of the Bias-Property of the Sample Auto-Correlation Matrices of Doubly Selective Fading Channels for OFDM Systems

Xiaochuan Zhao, Tao Peng, Ming Yang and Wenbo Wang
Wireless Signal Processing and Network Lab
Key Laboratory of Universal Wireless Communication, Ministry of Education
Beijing University of Posts and Telecommunications, Beijing, China
Email: zhaoxiaochuan@gmail.com

***Abstract*—In this paper, by assuming equiprobable centro-symmetric constellation adopted for modulation, the mathematic expectation of the sample auto-correlation matrix obtained through the least-squared channel estimation is derived under a rigorous model of the doubly selective fading channel for orthogonal frequency division multiplexing (OFDM) systems. Based on the derived expectation, the bias-property of the sample auto-correlation matrix is analyzed with respect to the total squared error (TSE) and the eigen-structure. And according to the analyses, when the sample auto-correlation matrix is used to estimate the signal and noise subspaces, BPSK may not be a good choice for modulation of pilot tones, which contradicts with the experience of most current OFDM systems. Numerical results demonstrate this bias-property and the analyses on it.**

***Index Terms*—Bias, Sample auto-correlation matrix, Doubly selective fading channels, OFDM, Total squared error, Eigen-structure.**

I. Introduction

The auto-correlation matrix of the channel frequency response (CFR) plays a very important role in the channel estimation for orthogonal frequency division multiplexing (OFDM) systems. Many channel estimation algorithms are based on this statistics, for example, the linear minimum mean-squared error (LMMSE) estimator and its optimal low-rank approximations [1], the MMSE estimator exploring both time and frequency correlations [2], the two-dimensional Wiener filtering [3], and those algorithms based on parametric channel modeling [4] [5] [6].

However, the true auto-correlation matrix of CFR is unknown in real applications, hence, the sample auto-correlation matrix is used in stead and usually obtained through the least squared (LS) channel estimation. For fixed or slowly moving radio channels whose Doppler spreads are relatively small, the channels reveal a feature of block-fading [7], which means the channels are static or nearly static intra-symbol. Under the circumstances, the sample auto-correlation matrix is unbiased if noise has not been involved. However, for fast moving radio channels, intra-symbol fading becomes so prominent that inter-carrier interference (ICI) takes effect by not only degrading the performance of OFDM systems [8], but also biasing the sample auto-correlation matrix. In [9], the bounds of the ICI power is derived.

In this paper, we focus on the bias-property of the sample auto-correlation matrix for OFDM systems in doubly selective fading channels. Based on an accurate channel modeling, we derive the mathematic expectation of the sample auto-correlation matrix by assuming equiprobable centro-symmetric constellations adopted for modulation. Further analyses, including the total squared error (TSE) and eigen-structure, are conducted thereafter.

This paper is organized as follows. In Section II, the OFDM system and channel model are introduced. Then, derivations of the bias of the sample auto-correlation matrix and related analyses are presented in Section III. Numerical results appear in Section IV. Finally, Section V concludes the paper.

Notation: Lowercase and uppercase boldface letters denote column vectors and matrices, respectively. $\odot$, $(\cdot)^*$, $(\cdot)^H$, and $||\cdot||_F$ denote Hadamard product, conjugate, conjugate transposition, and Frobenius norm, respectively. $E(\cdot)$ and $E_x(\cdot)$ represent the expectation and conditional expectation with respect to x, respectively. $[\mathbf{A}]_{i,j}$ and $[\mathbf{a}]_i$ denotes the (i,j)-th element of $\mathbf{A}$ and the i-th element of $\mathbf{a}$, respectively. $diag(\mathbf{a})$ is a diagonal matrix by placing $\mathbf{a}$ on the diagonal.

II. System Model

Consider an OFDM system with a bandwidth of $BW = 1/T$ Hz (T is the sampling period). N denotes the total number of tones, and a cyclic prefix (CP) of length L_{cp} is inserted before each symbol to eliminate inter-block interference. Thus the whole symbol duration is $T_s = (N + L_{cp})T$.

The complex baseband model of a linear time-variant mobile channel with L paths can be described by [10]

$$h(t,\tau) = \sum_{l=1}^{L} h_l(t)\delta\left(\tau - \tau_l T\right) \tag{1}$$

This work is sponsored in part by the National Natural Science Foundation of China under grant No.60572120 and 60602058, and in part by the national high technology researching and developing program of China (National 863 Program) under grant No.2006AA01Z257 and by the National Basic Research Program of China (National 973 Program) under grant No.2007CB310602.

where $\tau_l \in \mathcal{R}$ is the normalized non-sample-spaced delay of the l-th path, and $h_l(t)$ is the corresponding complex amplitude. According to the wide-sense stationary uncorrelated scattering (WSSUS) assumption, $h_l(t)$'s are modeled as uncorrelated narrowband complex Gaussian processes.

Furthermore, by assuming the uniform scattering environment introduced by Clarke [11], $h_l(t)$'s have the identical normalized time correlation function (TCF) for all l's, thus the TCF of the l's path is

$$r_{t,l}(\Delta t) = \sigma_l^2 J_0 \left(2\pi f_d \Delta t\right) \tag{2}$$

where σ_l^2 is the power of the l-th path, f_d is the maximum Doppler spread, and $J_0(\cdot)$ is the zeroth order Bessel function of the first kind. Additionally we assume the power of channel is normalized, i.e., $\sum_{l=0}^{L-1} \sigma_l^2 = 1$.

Assuming a sufficient CP, i.e., $L_{cp} \geq L$, the discrete signal model in the frequency domain is written as

$$\mathbf{y}_f(n) = \mathbf{H}_f(n)\mathbf{x}_f(n) + \mathbf{n}_f(n) \tag{3}$$

where $\mathbf{x}_f(n), \mathbf{y}_f(n), \mathbf{n}_f(n) \in \mathcal{C}^{N\times 1}$ are the n-th transmitted and received signal and additive white Gaussian noise (AWGN) vectors, respectively, and $\mathbf{H}_f(m) \in \mathcal{C}^{N\times N}$ is the channel transfer matrix with the $(k+\nu, k)$-th element as

$$[\mathbf{H}_f(n)]_{k+\upsilon,k} = \frac{1}{N}\sum_{m=0}^{N-1}\sum_{l=1}^{L} h_l(n,m) e^{-j2\pi(\upsilon m + k\tau_l)/N} \tag{4}$$

where $h_l(n,m) = h_l(nT_s + (L_{cp}+m)T)$ is the sampled complex amplitude of the l-th path. k and υ denote frequency and Doppler spread, respectively. Apparently, as $\mathbf{H}_f(n)$ is non-diagonal, ICI is present. In fact, when $f_d T_s \leq 0.1$, the signal-to-interference ratio (SIR) is over 17.8 dB [12].

III. Analysis of the Sample Auto-Correlation Matrix of the Channel Frequency Response

Usually the auto-correlation matrix of the channel frequency response is obtained through the LS channel estimation. For systems adopting pilot-symbol assisted modulation (PSAM) [1], only pilot symbols, denoted as $\mathbf{y}_p(n) \in \mathcal{C}^{N\times 1}$, are used to perform LS channel estimation. For systems employing data-aided channel estimation [13], all tones can be utilized to assist channel estimation if they have been demodulated. Then,

$$\begin{aligned}\mathbf{h}_{p,ls}(n) &= \mathbf{X}_p^{-1}(n)\mathbf{y}_p(n)\\ &= \mathbf{X}_p^{-1}(n)\mathbf{H}_p(n)\mathbf{x}_p(n) + \mathbf{X}_p^{-1}(n)\mathbf{n}_p(n)\end{aligned} \tag{5}$$

where $\mathbf{X}_p(n) = diag(\mathbf{x}_p(n))$ is a diagonal matrix consisting of pilot or demodulated symbols, and the noise term is $\mathbf{n}_p(n) \sim \mathcal{CN}(0, \sigma_n^2 \mathbf{I}_N)$.

The auto-correlation matrix of CFR referred in most literatures (see citations in section I) is assumed of the form as

$$\mathbf{R}_p = \mathbf{F}_{p,\tau}\mathbf{D}_p\mathbf{F}_{p,\tau}^H \tag{6}$$

where $\mathbf{F}_{p,\tau} \in \mathcal{C}^{N\times L}$ is the unbalanced Fourier transform matrix, defined as $[\mathbf{F}_{p,\tau}]_{k,l} = e^{-j2\pi k\tau_l/N}$. $\mathbf{D}_p \in \mathcal{C}^{L\times L}$ is a diagonal matrix with the l-th diagonal element $[\mathbf{D}_p]_{l,l} = \sigma_l^2$. In fact, $\mathbf{D}_p$ is the auto-correlation matrix of the channel impulse response (CIR).

TABLE I
VALUES OF ρ FOR TYPICAL MODULATIONS

Type of Modulation	BPSK	QPSK	16QAM	64QAM
ρ	1	1	1.889	2.685

With the LS estimated CFR $\mathbf{h}_{p,ls}(n)$, the sample auto-correlation matrix of CFR is constructed in most cases as

$$\hat{\mathbf{R}}_{p,ls} = \frac{1}{N_t}\sum_{n=1}^{N_t}\mathbf{h}_{p,ls}(n)\mathbf{h}_{p,ls}^H(n) \tag{7}$$

In most literatures, (7) is treated as an unbiased estimator of (6) when noise in not involved in the channel. However, substituting (5) into (7), we have (8), shown at the bottom of the next page, where N_t is the total number of observations. Therefore, its mathematic expectation is

$$E(\hat{\mathbf{R}}_{p,ls}) = \frac{1}{N_t}\sum_{n=1}^{N_t} E[\mathbf{h}_{p,ls}(n)\mathbf{h}_{p,ls}^H(n)] \tag{9}$$

By assuming that channel fading is independent of thermal noise, the additive term in (9) is

$$\begin{aligned}&E[\mathbf{h}_{p,ls}(n)\mathbf{h}_{p,ls}^H(n)] =\\ &\quad E[\mathbf{X}_p^{-1}(n)\mathbf{H}_p(n)\mathbf{x}_p(n)\mathbf{x}_p^H(n)\mathbf{H}_p^H(n)\mathbf{X}_p^{-H}(n)]\\ &\quad +\sigma_n^2 E[\mathbf{X}_p^{-1}(n)\mathbf{X}_p^{-H}(n)]\end{aligned} \tag{10}$$

In addition, we assume that the elements of $\mathbf{x}_p(n)$, $n = 1,\ldots,N_t$, are independent of each others, which is usually the case for pseudo-random pilot sequences or modulated data symbols. And so are the elements of $\mathbf{X}_p(n)$. Besides, we also assume a normalized centro-symmetric constellation set with equiprobability. Therefore,

$$E([\mathbf{x}_p(n)]_k) = 0 \tag{11}$$

$$E([\mathbf{x}_p(n_1)]_{k_1}[\mathbf{x}_p^*(n_2)]_{k_2}) = \delta(n_1-n_2)\delta(k_1-k_2) \tag{12}$$

$$E([\mathbf{x}_p(n_1)]_{k_1}^{-1}[\mathbf{x}_p^*(n_2)]_{k_2}^{-1}) = \rho\delta(n_1-n_2)\delta(k_1-k_2) \tag{13}$$

where ρ is a constant related to the type of modulation. For MPSK, $\rho = 1$, and for MQAM, ρ depends on the size of constellation, i.e.,

$$\begin{aligned}\rho = \frac{2(M-1)}{3M}&\sum_{k_1=0}^{\sqrt{M}-1}\sum_{k_2=0}^{\sqrt{M}-1}\\ &[(2k_1+1-\sqrt{M})^2 + (2k_2+1-\sqrt{M})^2]^{-1}\end{aligned} \tag{14}$$

where $M = 2^{2m}$, $m = 1, 2, \ldots$. Values of ρ for several typical modulations are evaluated in Table I.

For centro-symmetric constellations, according to (12) and (13), the first term on the right-hand side of (10) is expressed as follows through some manipulations (see Appendix A).

$$\begin{aligned}&E[\mathbf{X}_p^{-1}(n)\mathbf{H}_p(n)\mathbf{x}_p(n)\mathbf{x}_p^H(n)\mathbf{H}_p^H(n)\mathbf{X}_p^{-H}(n)] =\\ &\begin{cases}\mathbf{\Upsilon}\odot\mathbf{F}_{p,\tau}\mathbf{D}_p\mathbf{F}_{p,\tau}^H + (1-\xi_0)\rho\sigma_h^2\mathbf{I}_P, & \textit{BPSK}\\ \xi_0\mathbf{F}_{p,\tau}\mathbf{D}_p\mathbf{F}_{p,\tau}^H + (1-\xi_0)\rho\sigma_h^2\mathbf{I}_P, & \textit{others}\end{cases}\end{aligned} \tag{15}$$

where $\sigma_h^2 = \sum_{l=0}^{L-1} \sigma_l^2 = 1$, and ξ_0 is a scalar, defined as

$$\xi_0 = \frac{1}{N^2} \sum_{m=0}^{N-1} \sum_{q=0}^{N-1} J_0(2\pi f_d (m-q)T) \tag{16}$$

and $\boldsymbol{\Upsilon}$ is a Toeplitz matrix, defined as

$$[\boldsymbol{\Upsilon}]_{k_1,k_2} = \frac{1}{N^2} \sum_{m_1=0}^{N-1} \sum_{m_2=0}^{N-1} J_0(2\pi f_d (m_1 - m_2)T) \times e^{-j2\pi(k_1-k_2)(m_1+m_2)} \tag{17}$$

Substituting (13) into (10), the second term on the right-hand side of (10) is expressed as

$$\sigma_n^2 E[\mathbf{X}_p^{-1}(n)\mathbf{X}_p^{-H}(n)] = \rho\sigma_n^2 \mathbf{I}_N \tag{18}$$

With (15)(18)(10), (9) is rewritten into

$$E(\hat{\mathbf{R}}_{p,ls}) = \begin{cases} \boldsymbol{\Upsilon} \odot \mathbf{F}_{p,\tau}\mathbf{D}_p\mathbf{F}_{p,\tau}^H + [(1-\xi_0)\gamma + 1]\rho\sigma_n^2\mathbf{I}_N, & \textit{BPSK} \\ \xi_0\mathbf{F}_{p,\tau}\mathbf{D}_p\mathbf{F}_{p,\tau}^H + [(1-\xi_0)\gamma + 1]\rho\sigma_n^2\mathbf{I}_N, & \textit{others} \end{cases} \tag{19}$$

where $\gamma = \frac{\sigma_h^2}{\sigma_n^2}$ is the signal-to-noise ratio (SNR).

If considering the noise term presented in the LS estimation, the expected auto-correlation matrix, i.e., (6), should be modified to

$$\mathbf{R}_{p,ls} = \mathbf{F}_{p,\tau}\mathbf{D}_p\mathbf{F}_{p,\tau}^H + \rho\sigma_n^2\mathbf{I}_N \tag{20}$$

Compared with (20), (19) is no longer an unbiased estimator, and for most types of modulations except BPSK, its bias is

$$\begin{aligned} \Delta\mathbf{R} &= \mathbf{R}_{p,ls} - E(\hat{\mathbf{R}}_{p,ls}) \\ &= (1-\xi_0)\mathbf{F}_{p,\tau}\mathbf{D}_p\mathbf{F}_{p,\tau}^H - (1-\xi_0)\rho\sigma_h^2\mathbf{I}_N \end{aligned} \tag{21}$$

Hence, the corresponding TSE is defined as

$$\text{TSE}(\mathbf{R}_{p,ls}) \triangleq \|\Delta\mathbf{R}\|_F^2 = (1-\xi_0)^2 \sum_{l=1}^{L} (\lambda_l - \rho\sigma_h^2)^2 \tag{22}$$

where λ_l's are the eigenvalues of $\mathbf{R}_p$.

Although (7) reveals the property of bias, according to (19), using $E(\hat{\mathbf{R}}_{p,ls})$ to estimate the signal and noise subspaces is immune when BPSK is *not* adopted. In fact, let the eigenvalue decomposition (EVD) of $\mathbf{R}_{p,ls}$ is [14]

$$\mathbf{R}_{p,ls} = \mathbf{F}_{p,\tau}\mathbf{D}_p\mathbf{F}_{p,\tau}^H + \rho\sigma_n^2\mathbf{I}_N = \mathbf{U}\boldsymbol{\Gamma}\mathbf{U}^H$$

where $\mathbf{U}$ is unitary, and $\boldsymbol{\Gamma}$ is diagonal with $[\boldsymbol{\Gamma}]_{k,k} = \lambda_l + \rho\sigma_n^2$. Then, the EVD of $E(\hat{\mathbf{R}}_{p,ls})$ can be expressed as

$$E(\hat{\mathbf{R}}_{p,ls}) = \xi_0\mathbf{F}_{p,\tau}\mathbf{D}_p\mathbf{F}_{p,\tau}^H + [(1-\xi_0)\gamma+1]\rho\sigma_n^2\mathbf{I}_N = \mathbf{U}\hat{\boldsymbol{\Gamma}}\mathbf{U}^H$$

where $[\hat{\boldsymbol{\Gamma}}]_{k,k} = \xi_0\lambda_l + [(1-\xi_0)\gamma+1]\rho\sigma_n^2$, and $[\boldsymbol{\Gamma}]_{k,k} - [\hat{\boldsymbol{\Gamma}}]_{k,k} = (1-\xi_0)(\lambda_l - \rho\sigma_h^2)$. Therefore, only the eigenvalues are undermined by the interferences introduced by the doubly selective channels, leaving the corresponding eigenvectors unimpaired.

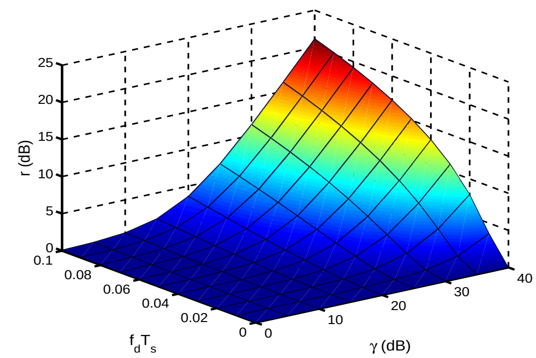

Fig. 1. Evaluating r versus f_dT_s and γ.

Nevertheless, if BPSK is adopted, not only the eigenvalues are undermined by the interference, but also the eigenvectors, of which the signal and noise subspaces consist, are deteriorated due to the presence of $\boldsymbol{\Upsilon}$.

Besides, from (19), we notice that the ICI caused by the doubly fading channels boosts the relative level of noise at a ratio of $r = \xi_0^{-1} + (\xi_0^{-1} - 1)\gamma = (1+\gamma)\xi_0^{-1} - \gamma$. Since when $f_dT_s \leq 0.1^*$, ξ_0 is a strictly monotonically decreasing function with respect to f_d, r is strictly monotonically increasing with respect to f_d, meanwhile, as $\xi_0 \leq 1$, r is strictly monotonically increasing with respect to γ. Fig.1 plots r versus f_dT_s and γ, where f_dT_s is the normalized Doppler.

IV. Numerical Results

The OFDM system in simulations is of $BW = 10$ MHz ($T = 1/BW = 100$ ns), $N = 1024$, and $L_{cp} = 128$. Two 3GPP E-UTRA channel models are adopted: Extended Vehicular A model (EVA) and Extended Typical Urban model (ETU) [15]. The excess tap delay of EVA is [0, 30, 150, 310, 370, 710, 1090, 1730, 2510] ns, and its relative power is [0.0, -1.5, -1.4, -3.6, -0.6, -9.1, -7.0, -12.0, -16.9] dB. For ETU, they are [0, 50, 120, 200, 230, 500, 1600, 2300, 5000] ns and [-1.0, -1.0, -1.0, 0.0, 0.0, 0.0, -3.0, -5.0, -7.0] dB, respectively. The classic Doppler spectrum, i.e., Jakes' spectrum [10], is applied to generate the Rayleigh fading channel.

In Fig.2, $N_t = 10^6$ OFDM symbols are collected to construct the sample auto-correlation matrix to approach its expectation. Three different types of modulation, including QPSK, 16QAM and 64QAM, are considered as well as a wide range of SNR's and Doppler's. It is shown that the numerical results coincide with the analytic results (22) rather well. According to the figure, TSE's for higher Doppler's are much

*This condition is implicit for applicable OFDM systems to maintain the power of ICI within a tolerable range [12].

$$\hat{\mathbf{R}}_{p,ls} = \frac{1}{N_t} \sum_{n=1}^{N_t} [\mathbf{X}_p^{-1}(n)\mathbf{H}_p(n)\mathbf{x}_p(n) + \mathbf{X}_p^{-1}(n)\mathbf{n}_p(n)][\mathbf{X}_p^{-1}(n)\mathbf{H}_p(n)\mathbf{x}_p(n) + \mathbf{X}_p^{-1}(n)\mathbf{n}_p(n)]^H \tag{8}$$

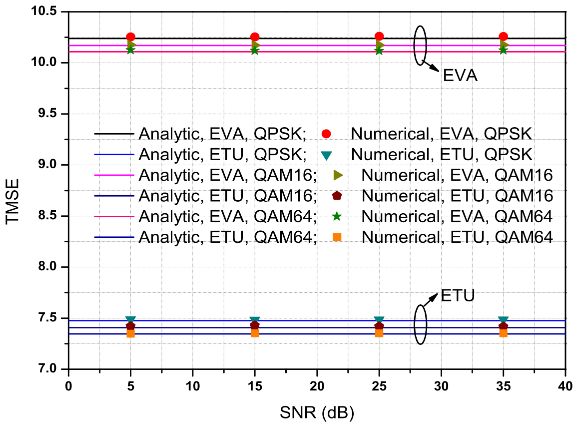

(a) $f_d = 600\text{Hz}$

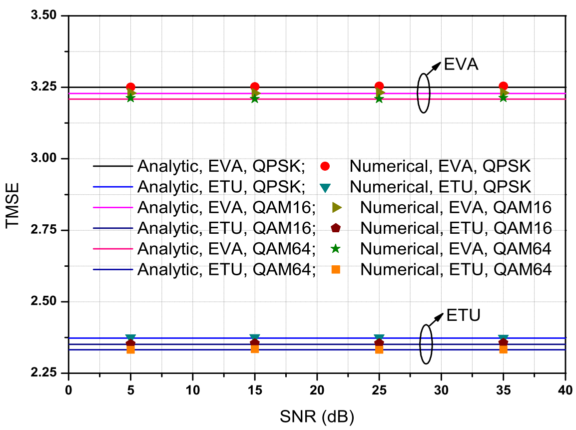

(b) $f_d = 450\text{Hz}$

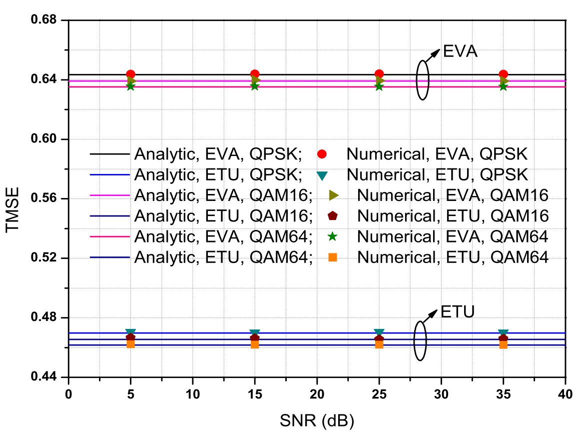

(c) $f_d = 300\text{Hz}$

Fig. 2. Evaluating TSE of the sample auto-correlation matrix for different modulations, Doppler's and SNR's when $N_t = 10^6$.

larger than lower ones, which follows (22) that $\|\Delta\mathbf{R}\|_F^2$ is strictly monotonically increasing with respect to f_d. Moreover, since $\frac{\partial\|\Delta\mathbf{R}\|_F^2}{\partial\rho} = -2(1-\xi_0)^2(N^2\sum_{l=1}^{L}\sigma_l^4 - L\rho) \leq 0$ for large N, TSE is decreasing with respect to ρ, which is demonstrated by the figure, too. Besides, for a given channel, the effect of different modulations on TSE is not as significant as of Doppler's.

V. Conclusion

In this paper, the bias-property of the sample auto-correlation matrix for OFDM systems in doubly selective fading channels is derived and analyzed. Through the analyses, it is found that the TSE of the sample auto-correlation matrix is increasing with respect to the Doppler but decreasing with respect to the order of modulation. Although the intra-symbol fading biases the expectation of the sample auto-correlation matrix, the eigenvectors are not affected at all when BPSK is not adopted, which allows subspace-based channel estimation algorithms. However, when BPSK is adopted, like most current OFDM systems did, not only eigenvalues but also eigenvectors are undermined by ICI due to the intra-symbol fading.

Appendix A
Derivation of (15)

Let $\mathbf{A} = \mathbf{X}_p^{-1}(n)\mathbf{H}_p(n)\mathbf{x}_p(n)\mathbf{x}_p^H(n)\mathbf{H}_p^H(n)\mathbf{X}_p^{-H}(n)$, then

$$[\mathbf{A}]_{k_1,k_2} = x_{k_1}^{-1}(n)x_{k_2}^{-*}(n)\sum_{q_1=1}^{N}\sum_{q_2=1}^{N}x_{q_1}(n)x_{q_2}^*(n)$$
$$\times\left(\frac{1}{N}\sum_{m_1=0}^{N-1}\sum_{l_1=1}^{L}h_{l_1}(n,m_1)e^{-j2\pi((k_1-q_1)m_1+k_1\tau_{l_1})/N}\right)$$
$$\times\left(\frac{1}{N}\sum_{m_2=0}^{N-1}\sum_{l_2=1}^{L}h_{l_2}(n,m_2)e^{-j2\pi((k_2-q_2)m_2+k_2\tau_{l_2})/N}\right)^*$$

Therefore

$$E\left([\mathbf{A}]_{k_1,k_2}\right) =$$
$$E_h\left\{\sum_{q_1=1}^{N}\sum_{q_2=1}^{N}E_x\left[x_{k_1}^{-1}(n)x_{k_2}^{-*}(n)x_{q_1}(n)x_{q_2}^*(n)\right]\right.$$
$$\times\left(\frac{1}{N}\sum_{m_1=0}^{N-1}\sum_{l_1=1}^{L}h_{l_1}(n,m_1)e^{-j2\pi((k_1-q_1)m_1+k_1\tau_{l_1})/N}\right)$$
$$\left.\times\left(\frac{1}{N}\sum_{m_2=0}^{N-1}\sum_{l_2=1}^{L}h_{l_2}(n,m_2)e^{-j2\pi((k_2-q_2)m_2+k_2\tau_{l_2})/N}\right)^*\right\}$$

With (11)-(13), we evaluate $E_x[\cdot]$ under the following cases.

1) When $k_1 = k_2 = q_1 = q_2 = k$,
$$E_x\left[x_k^{-1}(n)x_k^{-*}(n)x_k(n)x_k^*(n)\right] = 1$$

2) When $k_1 = k_2 = k, q_1 = q_2 = q, k \neq q$,
$$E_x\left[x_k^{-1}(n)x_k^{-*}(n)x_q(n)x_q^*(n)\right] = \rho$$

3) When $k_1 = q_1, k_2 = q_2, k_1 \neq k_2$,
$$E_x\left[x_{k_1}^{-1}(n)x_{k_2}^{-*}(n)x_{k_1}(n)x_{k_2}^*(n)\right] = 1$$

4) When $k_1 = q_2, k_2 = q_1, k_1 \neq k_2$,
$$E_x\left[x_{k_1}^{-1}(n)x_{k_2}^{-*}(n)x_{k_2}(n)x_{k_1}^*(n)\right] = \begin{cases}1, & \mathit{BPSK}\\ 0, & \mathit{others}\end{cases}$$

5) Others
$$E_x\left[x_{k_1}^{-1}(n)x_{k_2}^{-*}(n)x_{q_1}(n)x_{q_2}^*(n)\right] = 0$$

Note: To prove 4), let $x_{k_1}(n) = re^{j\theta}$, then $x_{k_1}^{-1}(n)x_{k_1}^*(n) = e^{-j2\theta}$. For equiprobable centro-symmetric constellations, θ and $-\theta$ are equiprobable, so $E_\theta(e^{-j2\theta}) = 0$ for all centro-symmetric constellations, e.g., MPSK ($M \neq 2$) and MQAM. Only for BPSK, $E_\theta(e^{-j2\theta}) = 1$.

According to 1) and 2), (23), shown at the bottom of this page, is obtained. Further, notice that

$$E_h[h_{l_1}(n,m_1)h_{l_2}^*(n,m_2)] = \sigma_{l_1}^2\delta(l_1-l_2)J_0(2\pi f_d(m_1-m_2)T)$$

(23) is expressed as

$$\begin{aligned} E\left([\mathbf{A}]_{k,k}\right) &= \rho\left(\sum_{l=1}^{L}\sigma_l^2\right)\left(\sum_{q=1}^{N}e^{j2\pi q(m_1-m_2)/N}\right) \\ &\times\left(\frac{1}{N^2}\sum_{m_1=0}^{N-1}\sum_{m_2=0}^{N-1}J_0(2\pi f_d(m_1-m_2)T)e^{-j2\pi k(m_1-m_2)/N}\right) \\ &+(1-\rho)\left(\sum_{l=1}^{L}\sigma_l^2\right)\left(\frac{1}{N^2}\sum_{m_1=0}^{N-1}\sum_{m_2=0}^{N-1}J_0(2\pi f_d(m_1-m_2)T)\right) \end{aligned}$$

Since $\sum_{q=1}^{N} e^{j2\pi q(m_1-m_2)/N} = N\delta(m_1-m_2)$, we have

$$E\left([\mathbf{A}]_{k,k}\right) = \rho\sigma_h^2 + (1-\rho)\sigma_h^2\xi_0 \tag{25}$$

where $\sigma_h^2 = \sum_{l=1}^{L}\sigma_l^2 = 1$, and ξ_0 is defined as

$$\xi_0 = \frac{1}{N^2}\sum_{m_1=0}^{N-1}\sum_{m_2=0}^{N-1}J_0(2\pi f_d(m_1-m_2)T)$$

Similarly, according to 3)-5), (24) is obtained and shown at bottom of this page. Therefore,

$$E\left([\mathbf{A}]_{k_1,k_2}\right) = \begin{cases} \upsilon_{k_1-k_2}\sum\limits_{l=1}^{L}\sigma_l^2 e^{-j2\pi(k_1-k_2)\tau_l/N}, & \textit{BPSK} \\ \xi_0\sum\limits_{l=1}^{L}\sigma_l^2 e^{-j2\pi(k_1-k_2)\tau_l/N}, & \textit{others} \end{cases} \tag{26}$$

where $k_1 \neq k_2$, and

$$\upsilon_{k_1-k_2} = \sum_{m_1=0}^{N-1}\sum_{m_2=0}^{N-1}J_0(2\pi f_d(m_1-m_2)T)e^{-j2\pi(k_1-k_2)(m_1+m_2)}$$

Consequently, with (25) and (26), we have

$$\begin{aligned} &E[\mathbf{X}_p^{-1}(n)\mathbf{H}_p(n)\mathbf{x}_p(n)\mathbf{x}_p^H(n)\mathbf{H}_p^H(n)\mathbf{X}_p^{-H}(n)] = \\ &\begin{cases} \boldsymbol{\Upsilon}\odot\mathbf{F}_{p,\tau}\mathbf{D}_p\mathbf{F}_{p,\tau}^H + (1-\xi_0)\rho\sigma_h^2\mathbf{I}_P, & \textit{BPSK} \\ \xi_0\mathbf{F}_{p,\tau}\mathbf{D}_p\mathbf{F}_{p,\tau}^H + (1-\xi_0)\rho\sigma_h^2\mathbf{I}_P, & \textit{others} \end{cases} \end{aligned}$$

where $\boldsymbol{\Upsilon}$ is a Toeplitz matrix, defined as $[\boldsymbol{\Upsilon}]_{k_1,k_2} = \upsilon_{k_1-k_2}$.

References

[1] O. Edfors, M. Sandell, J. van de Beek, S. Wilson, and P. Borjesson, "OFDM Channel Estimation by Singular Value Decompostion," *IEEE Trans. Commun.*, vol. 46, pp. 931–939, July 1998.

[2] Y. Li, L. Cimini, and N. Sollenberger, "Robust Channel Estimation for OFDM Systems with Rapid Dispersive Fading Channels," *IEEE Trans. Commun.*, vol. 46, pp. 902–915, July 1998.

[3] P. Hoeher, S. Kaiser, and P. Robertson, "Two-Dimensional Pilot-Symbol-Aided Channel Estimation by Wiener Filtering," in *IEEE ICASSP 1997*, April 1997, pp. 1845–1848.

[4] B. Yang *et al.*, "Channel Estimation for OFDM Transmission in Multipath Fading Channels Based on Parametric Channel Modeling," *IEEE Trans. Commun.*, vol. 49, pp. 467–479, March 2001.

[5] M. Raghavendra *et al.*, "Parametric Channel Estimation for Pseudo-Random Tile-Allocation in Uplink OFDMA," *IEEE Trans. Signal Process.*, vol. 55, pp. 5370–5381, November 2007.

[6] X. Zhao and T. Peng and W. Wang, "Parametric Channel Estimation by Exploiting Hopping Pilots in Uplink OFDMA," in *IEEE PIMRC 2008*, Cannes, France, September 2008.

[7] D. Shiu, G. Foschini, and M. Gans, "Fading Correlation and Its Effect on the Capacity of Multielement Antenna Systems," *IEEE Trans. Commun.*, vol. 48, pp. 502–513, March 2000.

[8] T. Wang *et al.*, "Performance Degradation of OFDM Systems Due to Doppler Spreading," *IEEE Trans. Wireless Commun.*, vol. 5, pp. 1422–1432, June 2006.

[9] Y. Li and L. Cimini, "Bounds on the Interchannel Interference of OFDM in Time-Varying Impairments," *IEEE Trans. Commun.*, vol. 49, pp. 401–404, March 2001.

[10] R. Steele, *Mobile Radio Communications*. IEEE Press, 1992.

[11] R. Clarke, "A Statistical Theory of Mobile Radio Reception," *Bell Syst. Tech. J.*, pp. 957–1000, July-Augeust 1968.

[12] Y. Choi, P. Voltz, and F. Cassara, "On Channel Estimation and Detection for Multicarrier Signals in Fast and Selective Rayleigh Fading Channels," *IEEE Trans. Commun.*, vol. 49, pp. 1375–1387, August 2001.

[13] V. Mignone and A. Morello, "CD3-OFDM: A Novel Demodulation Scheme for Fixed and Mobile Receivers," *IEEE Trans. Commun.*, vol. 44, pp. 1144–1151, September 1996.

[14] G. Golub and C. V. Loan, *Matrix Computations*, 3rd ed. New York: Johns Hopkins University Press, 1996.

[15] "3GPP TS 36.101 v8.2.0 – Evolved Universal Terrestrial Radio Access (E-UTRA); User Equipment (UE) Radio Transmission and Reception (Relasase 8)," 3GPP, May 2008.

$$\begin{aligned} E\left([\mathbf{A}]_{k,k}\right) = &\frac{\rho}{N^2}\sum_{q=1}^{N}\sum_{m_1=0}^{N-1}\sum_{l_1=1}^{L}\sum_{m_2=0}^{N-1}\sum_{l_2=1}^{L}E_h[h_{l_1}(n,m_1)h_{l_2}^*(n,m_2)]e^{-j2\pi[(k-q)(m_1-m_2)+k(\tau_{l_1}-\tau_{l_2})]/N} \\ &+\frac{1-\rho}{N^2}\sum_{m_1=0}^{N-1}\sum_{l_1=1}^{L}\sum_{m_2=0}^{N-1}\sum_{l_2=1}^{L}E_h[h_{l_1}(n,m_1)h_{l_2}^*(n,m_2)]e^{-j2\pi[k(\tau_{l_1}-\tau_{l_2})]/N} \end{aligned} \tag{23}$$

$$E\left([\mathbf{A}]_{k_1,k_2}\right) = \begin{cases} \frac{1}{N^2}\sum\limits_{m_1=0}^{N-1}\sum\limits_{l_1=1}^{L}\sum\limits_{m_2=0}^{N-1}\sum\limits_{l_2=1}^{L}E_h[h_{l_1}(n,m_1)h_{l_2}^*(n,m_2)]e^{-j2\pi[(k_1-k_2)(m_1+m_2)+k_1\tau_{l_1}-k_2\tau_{l_2}]/N}, & \textit{BPSK} \\ \frac{1}{N^2}\sum\limits_{m_1=0}^{N-1}\sum\limits_{l_1=1}^{L}\sum\limits_{m_2=0}^{N-1}\sum\limits_{l_2=1}^{L}E_h[h_{l_1}(n,m_1)h_{l_2}^*(n,m_2)]e^{-j2\pi(k_1\tau_{l_1}-k_2\tau_{l_2})/N}, & \textit{others} \end{cases} \tag{24}$$